

# Continental influence on the fertilization of marine waters during the late quaternary in the south of the Brazilian continental margin

Silvia Regina Bottezini<sup>1,\*</sup>, Débora Diniz<sup>2</sup>, Andréia Souza Pereira de Ávila<sup>3</sup>, Adriana Leonhardt<sup>2</sup>

<sup>1</sup> Universidade Federal do Rio Grande - Laboratório de Paleoceanografia e Palinologia - Programa de Pós-Graduação em Oceanologia (Av. Itália, km 8 - Cx. Postal: 474 - Bairro Carreiros - Rio Grande - 96201900 - RS - Brazil)

<sup>2</sup> Universidade Federal do Rio Grande - Instituto de Oceanografia - Laboratório de Paleoceanografia e Palinologia (Av. Italia km 8 - Cx. Postal: 474 - Bairro Carreiros - Rio Grande - 96201900 - RS - Brazil)

<sup>3</sup> Universidade Federal do Rio Grande do Sul - Laboratório de Geologia Costeira e Marinha - Programa de Pós Graduação em Geociências (Av. Bento Gonçalves, 9500 - Bairro Agronomia - Porto Alegre - 91501-970 - RS - Brazil)

\* Corresponding author: [silvia\\_bio@yahoo.com.br](mailto:silvia_bio@yahoo.com.br)

## ABSTRACT

This study sought to understand the role of continental influence on ocean productivity along the late Quaternary based on the comparison between continental palynomorphs and paleoproductivity proxies from the marine sediment core SIS188. Retrieved from the slope of the Pelotas Basin at a depth of 1,514 m, the core documents the time interval between 47.8 and 7.4 cal ka BP, including the Marine Isotope Stages (MIS) 3, 2 and 1. The palynological content found in the core SIS188 indicates a typical flora of the southern Brazil highlands, which is at the same latitude as the core. Thus, continental input sources, such as wind-borne dust and discharges from the Mampituba and Araranguá rivers, would more likely account for the palynological content than the Brazilian Coastal Current (BCC). During the glacial intervals (MIS 3 and MIS 2), paleoproductivity (indicated by the proxies coccolith numbers, N Ratio, and TOC content) suggest the intensification of upwelling and transport of wind dust, the latter of which may have transported pollen grains to the core region. There is a concentration decrease of continental palynomorphs at the end of MIS 2, which is accentuated during MIS 1 when the sea level is higher. Paleoproductivity was high during MIS 1, especially from the Holocene onwards, although the concentration of continental-derived palynomorphs decreases sharply, showing that the rise in sea level interferes with the fertilization of marine waters far from the coast by continental input.

**Descriptors:** Palynomorphs, Paleoproductivity, Continental influence, Pelotas basin, Brazilian Continental Margin.

## INTRODUCTION

Studies on paleoproductivity are of great importance, as they provide clues about past atmospheric and oceanographic systems variations. Continental margins are regions of high productivity due to high

nutrient input from continental influence and/or upwelling processes (Wang et al., 2015). The southern Brazilian margin is a productive area of the western margin of the South Atlantic due to two factors. The first is the South Atlantic upwelling system (20-28°S), currently located on the shelf and shelf break but which in the past may have undergone offshore expansion (Lessa et al., 2017). The other is fertilization through the La Plata River plume and continental drainage (Gonzalez-Silveira et al., 2006). Both

Submitted: 24-Aug-2021

Approved: 19-Apr-2022

Associate Editor: Fabrizio Frontalini



© 2022 The authors. This is an open access article distributed under the terms of the Creative Commons license.

represent important factors for the supply of nutrients to surface waters. Currently, the Brazilian Coastal Current (BCC), which transports the La Plata River plume (Piola et al., 2005), reaches latitudes of about 28°S, and its course to the north is mainly controlled as a function of wind tension (Piola et al., 2008).

Although various studies suggest an influence of BCC on the slope of the Brazilian Continental Margin (between 24.9° and 38°S) during glacial intervals, few use proxies linked to the plume of the La Plata River. One of these is Mathias et al. (2021), which characterized the sediments of the core GL-1090 collected in the Santos Basin (24° 92' S; 42° 51' W; at 2,225 m of water column). From paleomagnetic, geochemical (Al/Si and Fe/K), and grain size data, they derived a characterization compatible with La Plata River plume sediment. The authors concluded that the presence of these sediments on the slope was due to transport by BCC in glacial intervals with the lowest sea levels. However, it is also possible that these sediments were deposited at shallower depths and redistributed by undercurrents that also undergo changes with the decrease in relative sea level.

Other works that infer the presence of BCC in the open sea in the southern Brazilian Continental Margin present paleoproductivity proxies (Pivel et al., 2011 - planktonic foraminifera; Almeida et al., 2015 - benthic foraminifera; Gu et al., 2017; Gu et al., 2018a; Gu et al., 2018b – marine dinoflagellates) that could be responding to other fertilization mechanisms. On the other hand, Ávila et al. (2020), when studying palynomorphs and organic matter content in the sediments of the core REG972 (33.75S, 50.85W, 1,025 m of water column), attributed the increases in paleoproductivity in the Rio Grande cone region to a greater influence of Subantarctic Shelf Water during periods of lower sea level, rather than to the influence of BCC.

Therefore, the objective of this work is to analyze the role of continental influence on oceanic paleoproductivity in the south Brazilian Continental Margin during the period between 47.8 and 7.4 cal ka BP from the comparison of palynomorphs of continental origin and marine proxies for productivity.

## STUDY AREA

The marine sediment core SIS188 was collected on the northern continental slope of the Pelotas Basin (-29.221286; -47.283805, at 1,514 m water depth).

The sampling site is located approximately 206 km from the current coastline (Figure 1).

## CLIMATE AND ATMOSPHERIC CIRCULATION

In southern Brazil, the climate is humid temperate-subtropical, with evenly distributed rain throughout the year, relatively humid conditions, and annual precipitation of approximately 1,100 mm. El Niño Southern Oscillation (ENSO) events influence annual precipitation, showing positive anomalies during El Niño years and negative anomalies during La Niña years (Grimm and Tedeschi, 2009). Temperature varies throughout the year between 15 and 25°C (Diaz et al., 1998).

Atmospheric circulation in the study area is controlled by the high-pressure center of the South Atlantic anticyclone. The South Atlantic Subtropical High (SASH) is a high-pressure system located at approximately 30°S latitude over the Atlantic Ocean and associated with the southern mean meridional circulation of the atmosphere through the Hadley cell (Wainer and Taschetto, 2006; Moura et al., 2018). Variations in the intensity and position of SASH directly affect climate in South America and especially in Brazil. This system is responsible for the predominance of NE winds in the southwest region throughout the year and SW winds during the passage of cold fronts, more common during winter. The annual variability of the SASH is responsible for the seasonal migration of the BCC, which shifts north during the austral winter but is more restricted to the south during the summer (Bastos and Ferreira, 2000).

## OCEANOGRAPHIC CIRCULATION

The Brazil Current (BC) dominates the surface portion of the water column in the study area. The BC is the western contour current in the South Atlantic subtropical gyre and is responsible for heat and saltwater transport from the tropical region to higher latitudes in the Southwest Atlantic (Peterson and Stramma, 1991). It originates at approximately 10°S and comprises the southern branch of the South Equatorial Current (SEC), which bifurcates when reaching the coast of Brazil and rises to the North Brazil Current (NBC). The BC flows in a southerly direction, bypassing South America until reaching the region of the

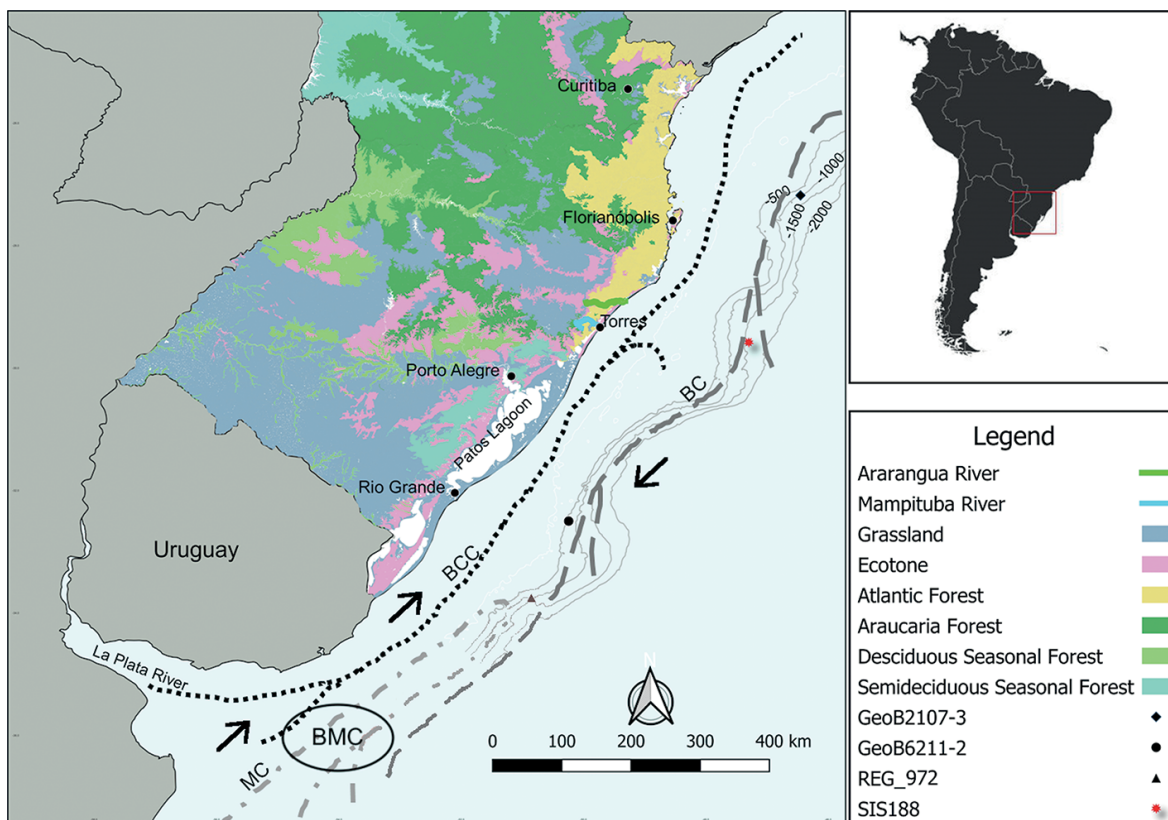


**Figure 1.** Location of SIS 188 core showing the main vegetation formations (IBGE, 2004) in the adjacent continental area and the oceanographic currents which influence the study area are indicated on the map (BC: Brazilian Current, BCC: Brazilian Coastal Current, MC: Malvinas Current, BMC: Brazil-Malvinas Confluence). The cores GeoB2107-3 (Gu et al., 2017), GeoB6211-2 (Gu et al., 2018a) and REG 972 (Ávila et al., 2020) are also indicated.

Brazil-Malvinas Confluence at ca. 38°S (Stramma and England, 1999). In the first 100 m, the BC transports Tropical Water (TW) with temperatures above 20°C, salinity > 36, and low nutrient concentrations (Peterson and Stramma, 1991; Stramma and England, 1999). Between depths of 100–600 m, the water column is dominated by South Atlantic Central Water (SACW), which is rich in nutrients and has temperatures ranging between 6–20°C and salinity between 34.6–36 (Braga and Nienschkeski, 2006).

The study area is also influenced by the Brazilian Coastal Current (BCC). The BCC is an arm of the BC that flows north along the coast and inner shelf, carrying nutrient-rich, low-temperature, and low-salinity waters as well as continental material from the La Plata River and the Patos Lagoon drainage basins (Souza and Robinson, 2004; Piola et al., 2005; Razik et al., 2015). The BCC can also carry sedimentary material from the

discharge of the Mampituba and Araranguá rivers, two smaller rivers that flow near the sampling area. The Mampituba River has a drainage area of 1,200 km<sup>2</sup> and an average flow of 18.6 m<sup>3</sup> s<sup>-1</sup> (D'Aquino et al., 2011). It begins in Serra Geral and flows into the Atlantic Ocean near the city of Torres, in the state of Rio Grande do Sul (Loitzembauer and Mendes, 2016). The watershed of the Araranguá River has an area of 3,020 km<sup>2</sup>, with an average flow of 65 m<sup>3</sup> s<sup>-1</sup>. It also begins in Serra Geral and flows into the Atlantic at the city of Araranguá (Loitzembauer and Mendes, 2016).

However, the main continental inputs to the Southwest Atlantic, the Patos Lagoon and the La Plata River, are located south of the sampling site. The Patos Lagoon has a surface area of 10,360 km<sup>2</sup> and is considered the largest choked lake in the world (Kjerfve, 1986). It receives water from a drainage basin of 140,000 km<sup>2</sup>, directly from tributaries, or through the São Gonçalo Channel, which

connects it with the Mirim Lagoon basin (Kjerfve, 1986). The La Plata River receives discharge from the La Plata drainage basin and is considered the second largest river system in South America, covering an area of approximately  $3.2 \times 10^6$  km<sup>2</sup> and extending along the coast for up to 1,300 km (Piola et al., 2005; Acha et al., 2008).

## REGIONAL GEOLOGY

The southern Brazilian continental shelf is quite extensive and is characterized by its smooth relief and low slope, with an average width of 125 km (Dias et al., 1994). In the northernmost part of the basin, next to SIS 188, the most pronounced feature is the Rio Grande Terrace, with bathymetry ranging from 250 to 500 m and occupying a considerable area of slope, estimated at around 500 km<sup>2</sup> (Basseto et al., 2000). Located further south of this basin is the Rio Grande Cone, a feature formed by a voluminous wedge of sediment resembling a cone and extending from the external shelf to depths of 4000 m (Basseto et al., 2000).

## VEGETATION

Various prior works describe the different types of vegetation present in southern Brazil and Uruguay (e.g., Klein, 1978, 1979; Boldrini, 2009; Oliveira-Filho et al., 2015), mainly influenced by the climate and topography of the region (Figure 1). The Atlantic Forest occupies the northern part of the southern region and the coastal plain. Coastal lagoons also occur along the coasts of the state of Rio Grande do Sul and Uruguay, dominated by marshlands composed mainly of the Cyperaceae, Chenopodiaceae, and Amaranthaceae families (Marangoni and Costa, 2009). In the higher portions, there is a mosaic of *Araucaria* forest and grasslands. *Araucaria* forests are found between 24° and 30°S and between 1,000 and 1,400 m of altitude (Hueck, 1966), and are mostly represented by *Araucaria angustifolia*, *Podocarpus lambertii*, *Mimosa scabrella*, *Ilex* spp., and *Dicksonia sellowiana* (Boldrini, 2009). The grasslands, which occupy vast areas of southern Brazil, are dominated by the Poaceae, Cyperaceae, Asteraceae, Apiaceae, and Fabaceae families, which are associated with cooler and drier climates (Mourelle and Prieto, 2012). Along the rivers and streams

of the region are riparian forests composed of the species *Salix chilensis*, *Sebastiania commersoniana*, *Myrsine laetevirens*, and others from the Myrtaceae family (Mourelle and Prieto, 2012).

## METHODS

The marine sediment core SIS188 (-29.221286; -47.283805) was extracted by Fugro from the northern continental slope of the Pelotas Basin at a water depth of 1,514 m, using a piston corer. A total of 338 cm of sediment was recovered. Approximately 20 cm from the upper and middle part of the core was removed, and the rest was sent to the Núcleo de Oceanografia Geológica of the Universidade Federal do Rio Grande (FURG) for refrigerated storage. The sedimentological description of the SIS188 core was presented by Petró et al. (2021).

## AGE MODEL

The age model was built based on the correlation between the  $\delta^{18}\text{O}$  isotopic curve of the planktonic foraminifera of the SIS188 core and the standard curve of Lisiecki and Stern (2016) (Figure 2). As control points, four AMS <sup>14</sup>C ages were obtained (Table 1). The age model was constructed using the AnlySeries software (Paillard et al., 1996) and was presented by Duque-Castaño et al. (2019) and Gonçalves and Leonhardt (2021a). Dating of <sup>14</sup>C was performed on the planktonic foraminifera *Globigerinoides ruber* (fraction > 150 μm; 10 mg per sample) using accelerated mass spectrometry (AMS) at the Laboratório de Radiocarbono of the Universidade Federal Fluminense (LAC-UFF). Ages derived from <sup>14</sup>C were adjusted considering a Delta R from the Marine Reservoir Correction Database of  $54.0 \pm 42.0$  (De Masi, 1999; Angulo et al., 2005; Alves et al., 2015) and calibrated according to the Marine13 curve (Reimer et al., 2013) using the Calib Radiocarbon Program (Stuiver and Reimer, 1993) (Table 1). Analyses of  $\delta^{18}\text{O}$  were also performed on *G. ruber* (fraction > 150 μm; 10-15 specimens per sample) in a MAT-253 dual input mass spectrometer with a Kiel IV carbonate device at the Laboratory of Stable Isotopes at the University of California, Santa Cruz. Isotope data are reported in permil against the Vienna Pee Dee Belemnite (V-PDB) standard (Figure 2).

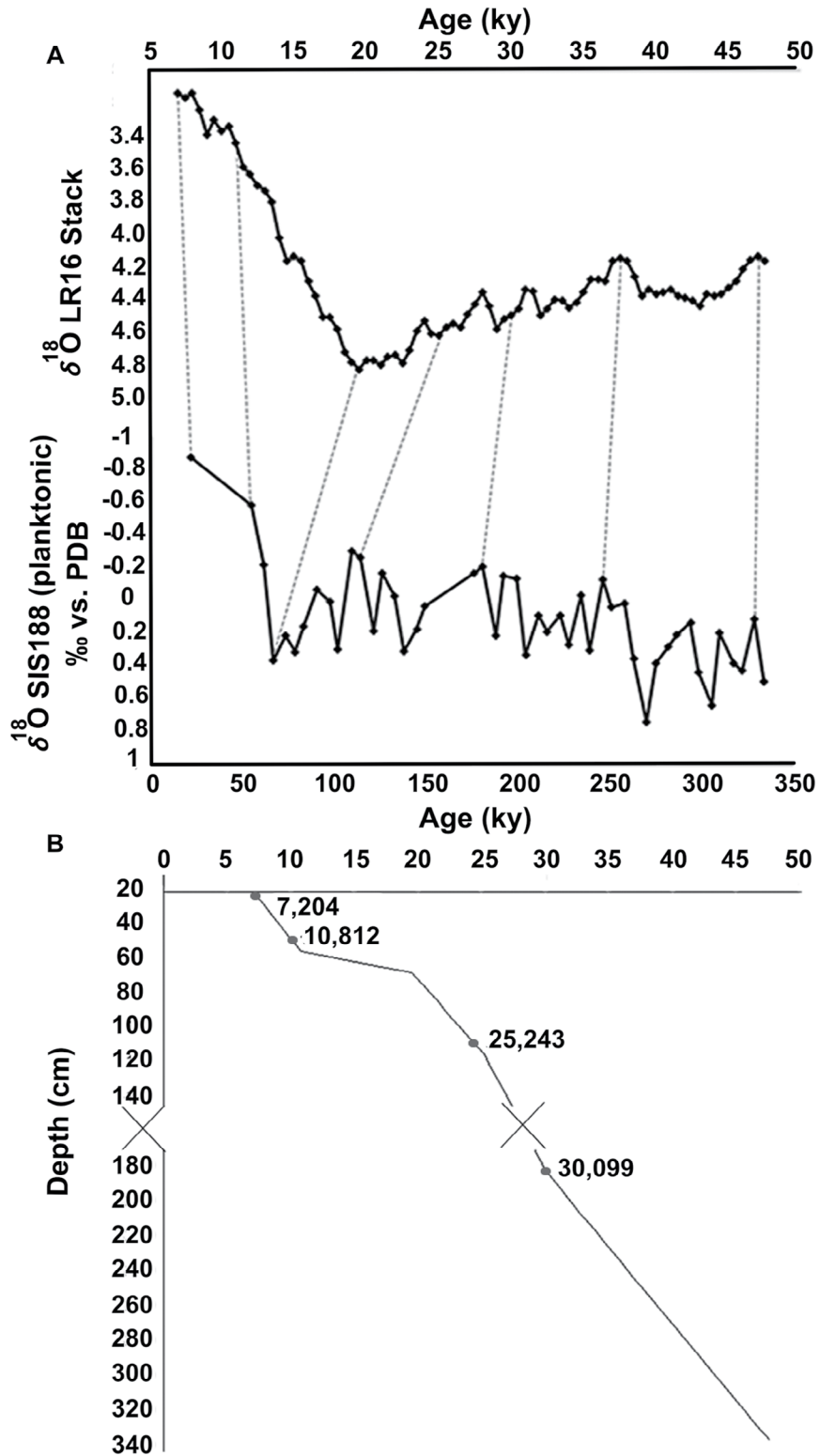


**Figure 2.** Age model of the core SIS188. (A) Correlation between Lisiecki and Stern (2016) South Atlantic intermediate standard curve and the oxygen isotope data from the marine core SIS188 (presented by Duque-Castaño et al. 2019). (B) Relationship between age and depth in the marine core SIS188. The dots are the depths where radiocarbon dating was performed.

**Table 1.** Radiocarbon ages used in the construction of the marine core SIS188 age model (Duque-Castaño et al. (2019); Gonçalves and Leonhardt (2021a)).

Depth (cm)	Species	Age ( <sup>14</sup> C years BP)	Error (years)	Calibrated age (cal ka BP)	Lab ID
21	<i>G. ruber</i>	6725	±31	7204	170210
54	<i>G. ruber</i>	9921	±34	10812	170055
113.5	<i>G. ruber</i>	21360	±59	25243	170056
180.8	<i>G. ruber</i>	26325	±77	30099	170211

## SAMPLE PROCESSING AND PALYNOLOGICAL ANALYSIS

For palynological analysis, 56 samples were collected at intervals of 6 cm along the core. Prior to processing, a tablet of the exotic spore *Lycopodium clavatum* (lot number 1030, produced by the Department of Quaternary Geology at Lund University, and calibrated in Sweden with  $20,848 \pm 1,545$  spores/tablet) was added to each sediment sample to calculate the concentration of pollen (Stockmarr, 1971). The palynological processing followed the preparation technique proposed by Faegri and Iversen (1975), with the addition of 10% hydrochloric acid (HCl) to remove carbonates and 5% potassium hydroxide (KOH) to remove organic matter and humic acids. To concentrate the palynomorphs, a solution of zinc chloride ( $ZnCl_2$ ) with a density between 1.8-1.9 g cm<sup>-3</sup> was used, and at least five slides of each sample were assembled in glycerinated gelatin. The slides were analysed under an optical microscope at 400x or 1,000x magnification, and 300 pollen grains and spores were counted for each sample when possible. Identification was based on several bibliographic references (e.g., Leal and Lorscheitter, 2007; Leonhardt and Lorscheitter, 2007, 2008, 2010; Roth and Lorscheitter, 2013; Masetto and Lorscheitter, 2016), as well as on the palynological collection in the laboratory.

Diatoms and dinoflagellates present on the palynological slides were also counted. Although these samples were not prepared for this purpose, these data were included as they provide interesting information when analysed with the pollen assemblage.

For paleoenvironmental interpretation purposes, taxa were grouped into the following categories: continental palynomorphs - Bryophytes, Pteridophytes, Herbs, Shrubs, Trees, Lianas, Varied Habits, Indeterminate (when the taxonomic identification of

the pollen grain was not possible) and Algae; marine palynomorphs - Palinoforminifera, Scolecodonts, Acritarchs and Dinoflagellates; and Diatoms.

## PALEOPRODUCTIVITY PROXIES

Paleoproductivity proxies (coccolith numbers, N ratio, and Total Organic Carbon (TOC) content) compared to palynological data were obtained by Gonçalves and Leonhardt (2021a), per the methodology below.

Samples of the SIS188 core were prepared using the technique of Koch and Young (2007) that enables an estimate of coccolith abundance per gram of dry sediment. At least 500 coccoliths were counted per sample using a petrographic microscope with 1000X magnification.

N ratio (Flores et al., 2000) based on coccolithophore algae was used to estimate the paleoproductivity and to monitor the nutricline depth variation. It consists of a ratio of the relative abundance of opportunistic species that benefit from enhanced nutrient availability in the upper photic zone (as *Gephyrocapsa* spp. and *Emiliania huxleyi*) and the species that inhabit the inferior photic zone and benefit from a deeper nutricline (as *Florisphaera profunda*).

Total Organic Carbon (TOC) in the sediments was measured through catalytic oxidation by combustion with a TOC-L Series SSM-5000<sup>a</sup> Shimadzu analyzer at the Laboratório de Análises Geoquímicas of Pontifícia Universidade Católica do Rio Grande do Sul (PUCRS). Approximately 30 mg of dry sediment was heated to 900°C in an oxygen rich environment, converting carbon to CO<sub>2</sub> detected by a gas infrared analyzer. To evaluate inorganic carbon, samples were acidified and oxidized at 200°C. The generated CO<sub>2</sub> is the inorganic carbon content of the sample. TOC concentration is defined by subtracting inorganic carbon

concentration from total carbon. Gonçalves and Leonhardt (2021a) also evaluated the carbonate content and sortable silt grain-size of sediments. The correlation between these proxies and TOC was not significant.

## STATISTICAL ANALYSIS

Percentages of continental palynomorphs (Bryophytes, Pteridophytes, Herbs, Shrubs, Trees, Lianas, Varied Habits, Indeterminate and Algae) were calculated using the total sum of the occurrence of these groups. The percentages of marine palynomorphs (Palynophoraminifera, Scolecodons, Acritarchs, and Dinoflagellates) were calculated using the sum of their occurrence and the total occurrence of continental palynomorphs. The percentage of diatoms was calculated using the sum of their occurrence and the total of continental and marine palynomorphs. The Tilia 2.1.1 software (Grimm, 1993) was used to construct pollen diagrams and to calculate sedimentation rates (clastic material), concentration, and percentage. All data were compared to the sea level curve, derived from the database available on the National Oceanic and Atmospheric Administration (NOAA) website (Spratt and Lisiecki, 2016), applicable worldwide. The standard deviation of this curve changes with time and is greatest between 8 and 22 cal ka BP, reaching > 10 meters at some ages.

The Pearson correlation coefficient was calculated between the N Ratio obtained by Gonçalves and Leonhardt (2021a) and the pollen concentration in the samples. The correlation significance was assessed by auto-resampling with 10,000 iterations and  $\alpha=0.1$ . Analyses used MULTIV statistical analysis software (Pillar, 1997).

Gonçalves and Leonhardt (2021b) calculated correlations between the paleoproductivity proxies (number of coccoliths per gram of sediment, N ratio, and TOC content in the sediment) and monthly insolation to 29°S over time (Laskar et al., 2004). Correlation significance was also assessed by auto-resampling with 10,000 iterations and  $\alpha=0.05$ . Analyses also used MULTIV statistical analysis software (Pillar, 1997).

## RESULTS

The marine sediment core SIS188 encompasses the time interval between 47.8 and 7.4 cal ka BP (Table 1, Figure 2).

In 56 analyzed samples, 40 spores and 59 pollen grains were identified, in addition to other non-pollen palynomorphs. Among continental indicators, the taxa related to the groups Herbs (27.7-67.2%), Varied Habits (0-60.6%), and Pteridophyte (1.9-18.7%) stand out. Among the marine indicators, the taxa *Spiniferites mirabilis* (0-4.2%), *Operculodinium centrocarpum* (0-2.9%), and *Cymatiosphaera* sp. (0-2.1%) stand out. The diatom species *Cyclotella meneghiniana* is also abundant through the core (0-25.3%) (Figure 3).

Results were divided by Marine Isotope Stages (MIS) documented in the marine core SIS188 for the purpose of paleoenvironmental interpretation. A detailed description main taxa fluctuations of the continental palynomorph groups can be obtained from Bottezini et al. (2021) (see [Supplementary Material](#)). Data on paleoproductivity obtained for the SIS188 core are also presented, as described in Gonçalves and Leonhardt (2021a).

The correlation between N Ratio and pollen concentration in the sediments was not significant ( $r=0.24$ ;  $\alpha=0.15$ ). However the correlation increases and becomes significant ( $r=0.33$ ;  $\alpha=0.07$ ) if samples corresponding to MIS 1 are removed.

### MIS 3 (47.7- 29 CAL KA BP; 336 - 176 CM)

This core interval is composed of carbonate-rich mud (Petró et al., 2021). Sedimentation rates are near 9 cm/kyr from 47.8 cal ka BP to around 30 cal ka BP. Thereafter, they reach 13.8 cm/kyr (highest value within the core) until the end of MIS 3 at 29 ka BP (Figure 3). Continental palynomorph concentrations are moderate in this interval until 29.8 cal ka BP ( $0-321.5 \times 10^4$  grains/cm<sup>3</sup>), increasing towards the end of MIS 3 and peaking at 28 cal ka BP ( $551.9 \times 10^4$  grains/cm<sup>3</sup>) (Figure 4).

Among continental indicators, "Herbs" predominate in MIS 3 (30.4-64%), followed by the "Varied Habits" (8-46.4%). "Bryophytes" (0-3.5%) and "Shrubs" (0-5.7%) were highest along the core in this interval. "Trees" (0-5.5%) showed decreased towards the end of the period. "Lianas" show low percentages throughout but increase slightly (2.6%) at 43 cal ka BP. The "Indeterminate" group shows a higher percentage (4.7-26.8%) within this range compared to subsequent ones, with peaks between 43 and 41.9 cal ka BP (14.7-24.7%) and between 37.5 and 35.9

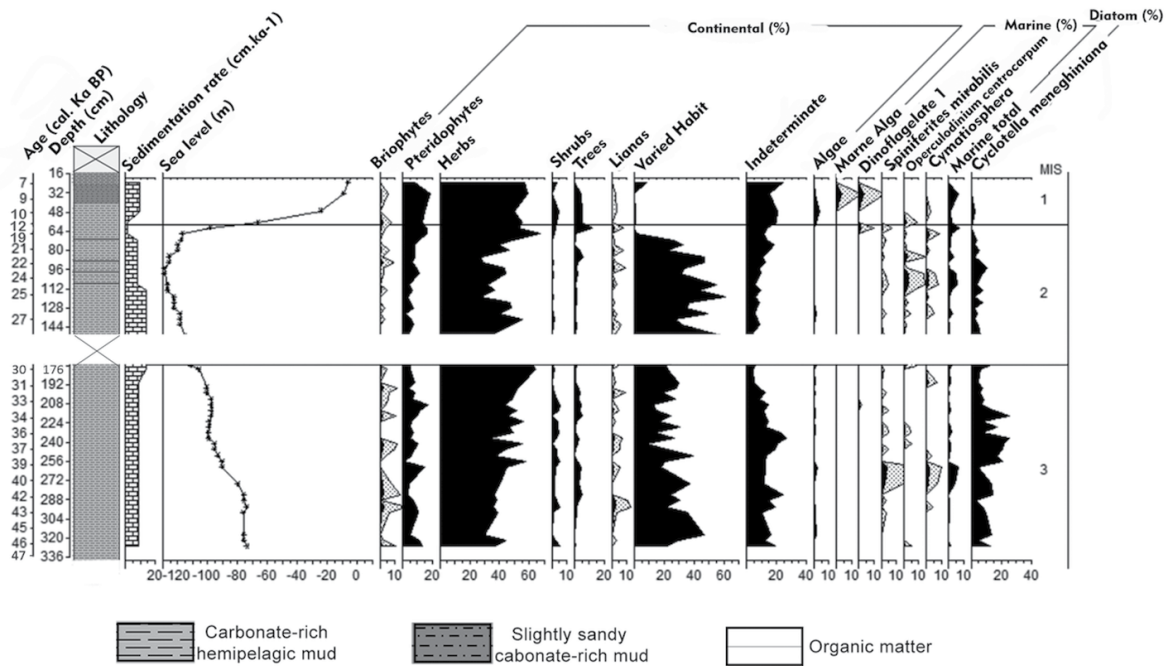


**Figure 3.** Pollen percentage summary showing lithology, sedimentation rate (in centimeters per thousand years), sea level (in meters; Spratt and Lisiecki, 2016), continental, marine, and diatom palynomorph groups, and Marine Isotope Stages (MIS). Briophytes, Lianas, Marine alga, Dinoflagellate, *S. mirabilis*, *O. centrocarpum* and *Cymatiosphaera* were exaggerated for better visualization.

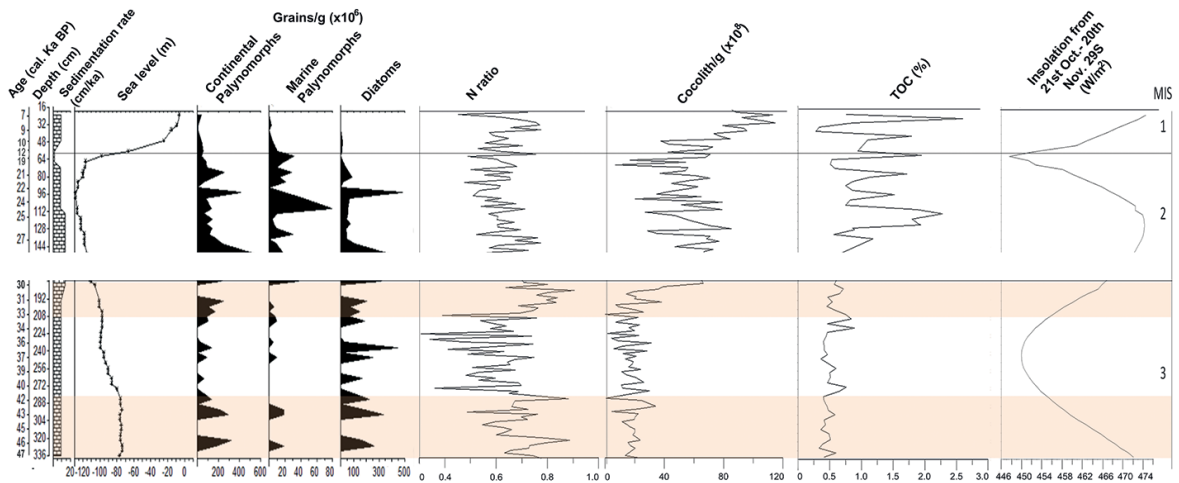


**Figure 4.** Sedimentation rate (in centimeters per thousand years), sea level (in meters; Spratt and Lisiecki, 2016), concentration of palynological indicators, paleoproductivity proxies (Gonçalves and Leonhardt, 2021a), and insolation at 29°S (Laskar et al., 2004). Shaded areas correspond to intervals of enhanced paleoproductivity related to higher dust influx (Gonçalves and Leonhardt, 2021b).

cal ka BP (19.2-26.8%). “Algae” have low percentages (0-2.2%), while the diatom *Cyclotella meneghiniana* has the highest values in this interval (3.4-25.3%) with higher proportions between 38.6-34.3 cal ka BP (7.4-25.3%) (Figure 3).

“Marine” concentrations are low throughout the MIS 3 (0-37 x 10<sup>4</sup> grains/cm<sup>3</sup>) (Figure 4), as are the percentages, despite a peak between 40.8 and 39.2 cal ka BP (reaching 6.3%), represented mainly by the dinoflagellate *Operculodinium*

*centrocarpum* and the algae *Cymatiosphaera* sp. (Figure 3).

According to Gonçalves and Leonhardt (2021a), the curve of coccoliths per gram of sediment shows low values ( $0-66.3 \times 10^8$  coccolith/g) for nearly the entire MIS 3, increasing from 30.1 ka. Likewise, the TOC curve shows the lowest recorded values in the core (0.33-0.89 %). Unlike prior proxies, the N Ratio curve does not show particularly low values throughout MIS 3; increased N Ratio intervals are noted between 47.5 - 41.7 cal ka BP and 33.3 - 29.9 cal ka BP (Gonçalves and Leonhardt, 2021a) (Figure 4).

### MIS 2 (29 - 14 CAL KA BP; 176 - 59 CM)

In this interval, sediments are composed of carbonate-rich mud with thin layers of organic matter at depths of 75, 90, 100, and 105 cm (Petró et al., 2021). Sedimentation rates at the beginning of MIS 2 are high (13.8 cm/kyr) up to 24.9 cal ka BP, at which point they drop to 8.3 cm/kyr. At 19.5 cal ka BP, sedimentation rates are even lower, reaching the minima for the studied interval (1.4 cm/kyr) (Figure 3).

The concentrations of most palynomorphs of continental origin are high in MIS 2. However, the concentrations of “Bryophytes” and “Shrubs” are very low ( $0-18.6 \times 10^4$  and  $0-24.8 \times 10^4$  grains/g, respectively). There is a concentration peak at 22.9 cal ka BP of the “Continental palynomorphs” curve ( $407 \times 10^4$  grains/g, with emphasis on the groups “Pteridophytes”, “Herbs,” “Trees,” and “Lianas”), also seen in the “Diatoms” curve ( $48.3 \times 10^4$  grains/g) (Figure 3).

Among continental indicators, “Varied Habits” (0-60.6 %) and “Herbs” (27.6-67.2%) continue to prevail in the record, the former predominating. However, at the end of MIS 2, the percentages of “Varied Habits” drop abruptly, and “Herbs” once again dominate pollen association. The percentages of “Pteridophytes” tend to increase beginning at 27.3 cal ka BP, especially between 19.5-15.9 cal ka BP, reaching 16.4%. “Trees” show an increase in percentage between 22.4-21.2 cal ka BP and a peak at 15.9 cal ka, reaching 11.9%. “Bryophytes,” “Lianas,” and “Shrubs” continue to show low percentages. “Indeterminate” shows lower percentages than in MIS 3 (3-18.5%),

increasing towards the end of MIS 2. “Algae” present lower percentages than in MIS 3 (0-1.3%). *C. meneghiniana* percentages decline compared to MIS 3 (0-10.6%) (Figure 3).

“Marines” reach their highest concentration in MIS 2 ( $0-79 \times 10^4$  grains/g), with peaks at 29.8, 26.6, 24.7, and 15.9 cal ka BP (Figure 4). The percentages range from 0 to 6.9%, with peaks between 24.7-23.6 cal ka BP and at 15.9 cal ka BP, with an emphasis on *O. centrocarpum* and *Cymatiosphaera* (Figure 3).

According to Gonçalves and Leonhardt (2021a), the curve of coccoliths per gram of sediment shows a slight decrease from the beginning of MIS 2 to the end of UMG ( $6.9-85.3 \times 10^8$  coccolith/g), increasing later. TOC clearly increases compared to MIS 3 values but with greater fluctuations, reaching the highest levels between 25.9-24.8 cal ka BP (1.8 to 2.28%) and the lowest between 20.3-18.3 cal ka BP (0.51 to 0.58%). The N Ratio decreases over MIS 2 (Gonçalves and Leonhardt, 2021a) (Figure 4).

### MIS 1 (14 - 7.4 CAL KA BP; 59 - 22 CM)

Over most of this interval, sediments are composed of carbonate-rich hemipelagic mud, except for between 31-45 cm which contains a lightly sandy carbonate-rich mud (Petró et al., 2021). Sedimentation rates increase from 1.4 cm/kyr to 9.1 cm/kyr beginning at 10.8 cal ka BP (54 cm) (Figure 3).

The concentrations of palynomorphs of continental origin are very low during MIS 1 ( $4.1-54.7 \times 10^4$  grains/g) (Figure 4). “Herbs” dominate the pollen association (49.7-59.1%), but “Pteridophytes,” “Trees,” and “Shrubs” are also significant. The percentages of “Varied habits,” “Bryophytes,” and “Lianas” remain low. The “Indetermined” group has high percentages (15.5-24.2%) in this range. “Algae” percentages are slightly higher, between 12.6-10 cal ka BP (1.5-3.6 %). The diatom *C. meneghiniana* shows its lowest percentage during MIS 1 (0-2.8%) (Figure 3).

“Marine” concentrations also drop at the beginning of MIS 1 ( $0-10.3 \times 10^4$ ) (Figure 4), although their percentages peak at 6.8% at 8.5 cal kyr BP. The specimens *O. centrocarpum* and *Cymatiosphaera* do not stand out during MIS 1 (Figure 3).

According to Gonçalves and Leonhardt (2021), the highest content of coccoliths per gram of sediment are found in MIS 1, during the Holocene, reaching  $115 \times 10^8$  coccoliths/gram at 8.5 cal ka BP. TOC shows its highest and lowest levels during the Holocene, ranging from 0.28% (9.1 cal ka BP) to 2.6% (7.9 cal ka BP). The N Ratio curve increases during the Holocene, especially between 9 and 7.9 cal ka BP (Gonçalves and Leonhardt, 2021a) (Figure 4).

## DISCUSSION

The primary productivity of the Southwest Atlantic region can be increased by several local factors such as the position of the Brazil-Malvinas Confluence, a greater influence of the La Plata River plume (transported by the BCC), the strengthening of upwelling systems, and the intensification of the westerly winds that carry continental dust to the ocean. It is known that the Brazil-Malvinas Confluence is a region of high productivity that migrates seasonally, going to the south during the austral summer and to the north during the austral winter. Over Quaternary, this migration may have been wider, driven by changes in the intensity of the westerly winds. However, after studying three cores at the Confluence area, Voight et al. (2015) concluded that its migration never exceeded the range of 32.5-39.3°S during the Holocene. Gu et al. (2019) found evidence of the Confluence influence in a core at 38,018°S, which decreases to the north and is not perceived at the SIS188 core latitude (Gu et al., 2017; 2018). Thus, the migration of the Brazil-Malvinas Confluence does not seem to be responsible for the increase in productivity in our record, nor for the transport of continental palynomorphs to the region.

Recently, several studies have pointed to the BCC as one of the main agents redistributing terrigenous sediments and fertilizing marine waters in the region, both on the continental shelf or in the open ocean (Mahiques et al., 2009; Pivel et al., 2011; Mathias et al., 2014; Gu et al., 2017; Gu et al., 2018; Mathias et al., 2020). The BCC, though currently a coastal current, would influence the slope region at intervals where the relative sea level was lower (Pivel et al., 2011; Gu et al., 2017; Gu et al., 2018; Mathias et al., 2020).

However, a study on paleoproductivity carried out in the core SIS188 (Gonçalves and Leonhardt, in press) found a clearer relationship of the proxies N ratio, coccoliths/g, and TOC content in sediments (Gonçalves and Leonhardt, 2021a) with the insolation of the study area (Laskar et al., 2004) (Figure 4), which drives the SASH and, consequently, the BC, the BCC, and upwelling systems.

Insolation drives atmospheric processes and can play an important role in enhancing or weakening upwelling systems. The SASH is currently shifted south between January and March, causing northeasterly winds to predominate in the southern and southeastern regions of Brazil during the austral summer, intensifying upwelling (Palma and Matano, 2009), and causing the plume of the La Plata River to be contained to the south. During winter, there is a predominance of southwest winds in the region, which drive the plume to the latitude of the study region (Piola et al., 2005).

The same mechanism may have occurred over time in the region's recent past. The correlation between different paleoproductivity proxies (N Ratio, coccoliths/g, and TOC content in sediments) from the core SIS188 with the monthly insolation over time (Figure 4), demonstrated by Gonçalves and Leonhardt (2021b), shows a pattern similar to the current one for the time interval studied, with positive correlation during spring and early summer and negative correlation during late summer and early autumn. Therefore, the increase in productivity in the study area increases at intervals of higher insolation with a predominance of northeasterly winds, which intensify upwelling. No significant correlations were found for the intervals of lower insolation (austral winter), when the BCC could reach the latitude of the study area driven by southwest winds (Gonçalves and Leonhardt (2021b)).

Furthermore, the palynological content found in the core SIS188 points to the presence of several elements of the *Araucaria* forest (Bottezini et al., 2021 - see [Supplementary Material](#)), a typical vegetation of the East Plateau of RS, which is at the same latitude as the core. The exotic pollen grains *Alnus* sp. and *Nothofagus* sp. are very scarce in the core SIS188, indicative of long-distance transport. Both are typical of Andean vegetation

(Cabrera, 1994) and could have reached the study area by wind transport, since these are also found in bogs on the South Brazilian Plateau (Leonhardt and Lorscheitter, 2009). Other than wind-borne dust, sources of continental input to the ocean include the discharges from the Mampituba and Araranguá rivers. The correlation analysis between pollen concentration in the sediments and N-Ratio found in the core SIS188 indicates some influence of continental input on fertilization of the marine environment in the studied area. However, this correlation ( $r = 0.33$ ) is only significant when samples belonging to MIS 1 are excluded from the analysis, suggesting that the rise in sea level hinders the arrival of these elements in the open sea.

However, the fossil record may also reflect processes that occurred after the arrival of palynomorphs on the seabed due to sediment removal by the deep current. Gonçalves and Leonhardt (2021a) measured the size of the sortable silt in SIS188 samples, which is considered a proxy for the deep current velocity. Although the analyses they carried out were not on the same samples used in this work, one notes a slight tendency of greater concentration of palynomorphs during the time intervals in which the Intermediate Western Boundary Current (IWBC) was presumably slower (Gonçalves and Leonhardt, 2021a). As such, a portion of the fluctuation in concentration of palynomorphs in the sediments may be due to changes in the velocity of the IWBC, in addition to the changes in the palynomorph influx in the studied area.

### **MIS 3 (47.7- 29 CAL KA BP, 336 - 137.5 CM)**

The climate during this interval was predominantly cold (with a predominance of grassland vegetation, indicated by the high percentages of “Herbs”). Climatic conditions were sufficiently wet for the development of lakes and swamps on the coastal plain (indicated by high percentages of “Bryophytes,” “Pteridophytes,” and the diatom *C. meneghiniana*) and of forest formations probably in refuges (Figure 3) (Bottezini et al., 2021 – see [Supplementary Material](#)).

During MIS 3, paleoproductivity (inferred by N ratio) was higher between 47.5–41.7 ka BP and 33.3–29.9 ka BP in the core SIS188 (Figura

4) (Gonçalves and Leonhardt, 2021a; Gonçalves and Leonhardt, (2021b)). These intervals coincide in part with the increase in dust influx followed by the increase in productivity found in the core SIS249 (Lopes et al., 2021), which is very close to SIS188. The authors attribute this increase in dust influx to the expansion to the north of the southwest wind belt generated by the South Pacific anticyclone during glacial intervals (Pichat et al., 2014; Jacobel et al., 2017), reaching the Pelotas Basin. These intervals of higher productivity associated with dust influx contain the samples that reach the highest pollen concentrations of MIS 3 (Figure 4), suggesting that these palynomorphs arrived by wind transport.

The positive correlation between pollen concentration in sediments and the N-Ratio ( $r = 0.33$ , excluding MIS 1) is consistent with this explanation. The same pattern was not observed for the other paleoproductivity proxies (coccolith abundance and TOC content in sediments), which may be due to changes in deep water chemical properties (for example, pulses of more oxygenated waters during glacial periods could degrade organic matter) (Gonçalves and Leonhardt, 2021a). It may also be related to changes in deep current velocity (lower velocities allow for a higher sedimentation rate and dilution of coccoliths in the sediments), as indicated by changes at sortable silt mean size in SIS188 core (Gonçalves and Leonhardt, 2021a).

### **MIS 2 (29 - 14 CAL KA BP, 137.5 - 59 CM)**

During MIS 2, climatic fluctuations induced changes in the ecological structure of vegetation (increase in “Varied Habits”), with environmental conditions starting to become drier and cooler (decrease in the percentages of *C. meneghiniana* and “Trees,” “Bryophytes,” and “Pteridophytes”) (Figure 3). This climatic trend becomes more evident around 19.5 cal ka BP, during the Last Glacial Maximum (LGM) (Bottezini et al., 2021 – see [Supplementary Material](#)). It is interrupted at 15.9 cal ka BP, possibly due to the Heinrich Event 1, which is characterized by greater precipitation and/or a temperature increase (Bottezini et al., 2021 - see [Supplementary Material](#)).

The increase in proxies such as coccolith per gram of sediment and TOC content is quite

accentuated and remains so throughout MIS 2, demonstrating the increase in paleoproductivity at this stage related to the intensification of upwelling in the region (Pereira et al., 2018; Gonçalves and Leonhardt, (2021b)). This may have been accompanied by changes in the deep water chemical properties [with less significant occurrences of oxygenated waters pulses, allowing organic matter to be preserved (Gonçalves and Leonhardt, 2021a)]. However, the deep current velocity does not seem to have changed in the beginning of MIS 2 (Gonçalves and Leonhardt, 2021a), suggesting that the increased coccolith numbers are related to a significant increase in population. Although palynomorph concentrations show a surge at the start of MIS 2, they do not sustain these high levels throughout the stage although they are, on average, higher than during MIS 3 and MIS 1 (Figure 4). This increase in concentration of continental palynomorphs may be related to the core's greater proximity to the coastline and of mouths of the Araranguá and Mampituba rivers due to the lowering of the sea level and/or the intensification of winds during MIS 2, especially during the LGM (Kohfeld et al., 2013).

The decrease in sea level characteristic of MIS 2 is also reflected in the record of marine palynomorphs, which reach their highest concentrations during this interval mainly due to the occurrence of *O. centrocarpum* and *Cymatiosphaera* sp. Associated with the coastal-ocean transition (Dale, 1996; Zonneveld et al., 2013), *O. centrocarpum* is a cosmopolitan dinoflagellate that can occur in environments with high salinity and low levels of nutrients. This species is commonly found in sediment under warm water bodies such as the Tropical Water, which is transported by the BC (Santos et al., 2017). The algae *Cymatiosphaera* sp. is understood to be an indicator of neritic environments (Grill and Quatrocchio, 1996), with a greater proportion in the core SIS188 when the sea level was lower.

There is a significant reduction in the sedimentation rate at the end of MIS 2 and beginning of MIS 1 (between 19.5-12.6 cal ka BP), possibly related to deglaciation and an increase in the relative sea level, displacing the mouth of the Mampituba and Araranguá rivers, which begin to deposit sediment in shallower waters, possibly leading to the

decrease in concentration of most palynomorphs (which extends to the end of the record).

### MIS 1 (14 - 7.4 cal ka BP; 59 - 22 cm)

With the climatic changes of deglaciation and the beginning of the Holocene, a small development of forests and lakes is observed on the continent, while grasslands remain the dominant plant formation (Figure 3) (Bottezini et al., 2021 – see [Supplementary Material](#)).

The decrease in concentration of continental palynomorphs observed since the end of MIS 2 is accentuated during MIS 1, when the sea level is higher (causing the retrogradation of the coastline, which enables the retention of sediments and palynomorphs on the coast) and the southern westerly winds are weakened during the Holocene (Voigt et al., 2015), decreasing wind transport of palynomorph to the study area.

According to paleoproductivity proxies measured in the core SIS188 (Figure 4), the paleoproductivity was high during MIS 1, especially during the Holocene (Gonçalves and Leonhardt, 2021a). Since the upwelling system seems to be weakened during this interval (Chiessi et al., 2015; Pereira et al., 2018; Duque-Castaño et al., 2019; Gonçalves and Leonhardt, (2021b)), this higher productivity could be the result of geochemical dynamics caused by marine regression during the LGM (Gonçalves and Leonhardt, (2021b)). Filippelli et al. (2007) demonstrated that the redistribution of phosphorus from the continental margin to the deep ocean during marine regressions can show a lag of 10-20 kyr between the phosphorus-based export production records and the sea level change, causing the maximum increase in productivity to be noticed only during deglaciation. At the same time, the concentration of palynomorphs of continental origin decreases significantly during this interval, demonstrating a decoupling of continental input (be it wind or fluvial) and marine productivity. The correlation between the N-Ratio and the pollen concentration in the sediments only becomes significant once samples of this MIS are excluded, also pointing to the rise in sea level as a factor that interferes with the fertilization of marine waters far from the coast by continental input.

## CONCLUSION

The studied core covered the time interval between 47.8-7.4 cal ka BP, recording part of MIS 3, MIS 2, and part of MIS 1. The palynological association found along the SIS188 core indicates a source area compatible with the vegetation of grasslands and *Araucaria* forest typical of the southern Brazil highlands. There are no palynological indicators of the influence of BCC in our record. Comparison of continental palynomorphs with paleoproductivity proxies in the core SIS188 indicates that BCC did not have a clear influence on the fertilization of marine waters. The concentration of palynomorphs in the sediments seems to be controlled by the velocity of the deep water current, the intensity of the winds, and the rise and fall of the sea level (these last two factors lead to increased paleoproductivity during the glacial interval - MIS 3 and MIS 2).

## ACKNOWLEDGMENTS

The authors thank CAPES - Brazil (Coordenação de Aperfeiçoamento de Pessoal de Nível Superior - Brasil) for the financial support (CAPES process nº 88887.091729/2014-01) and for the doctoral scholarship that made this work possible. The first author is also grateful to the Programa de Pós Graduação em Oceanologia of Universidade Federal do Rio Grande (FURG) for the opportunity.

## AUTHOR CONTRIBUTIONS

S.R.B.: Conceptualization; Investigation; Formal analysis; Writing - original draft; Writing - review & editing;

D.D.: Visualization;

A.S.P.A.: Visualization;

A.L.: Supervision; Resources; Project Administration; Funding Acquisition; Writing - original draft; Writing - review.

## REFERENCES

- ACHA, E. M., MIANZAN, H., GUERRERO, R., CARRETO, J., GILBERTO, D., MONTOYA, N. & CARIGNAN, M. 2008. An overview of physical and ecological processes in the Río de la Plata Estuary. *Continental Shelf Research*, 28(13), 1579-1588.
- ALMEIDA, F. K., MELLO, R. M., COSTA, K. B. & TOLEDO, F. A. L. 2015. The response of deep-water benthic foraminiferal assemblages to changes in paleoproductivity during the Pleistocene (last 769.2 kyr), western South Atlantic Ocean. *Palaeogeography, Palaeoclimatology, Palaeoecology*, 440, 201-212.
- ALVES, E., MACARIO, K., SOUZA, R., PIMENTA, A., DOUKA, K., OLIVEIRA, F., CHANCA, I. & ANGULO, R. 2015. Radiocarbon reservoir corrections on the Brazilian coast from pre-bomb marine shells. *Quaternary Geochronology*, 29, 30-35.
- ANGULO, R. J., SOUZA, M. C., REIMER, P. J. & SASAKA, S. K. 2005. Reservoir effect of the Southern and Southeastern Brazilian Coast. *Radiocarbon*, 47, 67-73.
- ÁVILA, A. S. P., LEONHARDT, A. & DINIZ, D. 2020. Paleoenvironmental reconstruction off southern Brazil during a glacial period (66.5-47 kyr BP): continental and oceanic environments. *Journal of Coastal Research*, 36, 1204-1214.
- BASSETTO, M., ALKMIM, F. F., SZATMARI, P. & MOHRIAK, W. U. 2000. The oceanic segment of the southern Brazilian margin: morpho-structural domains and their tectonic significance. In: MOHRIAK, W. U. & TALWANI, M. (eds.). *Atlantic rifts and continental margins*. Washington: AGU (American Geophysical Union), pp. 235-259.
- BASTOS, C. C. & FERREIRA, N. J. 2000. Análise climatológica da alta subtropical do Atlântico Sul. In: Anais do XI Congresso Brasileiro de Meteorologia (CBMET), 2000 Oct 16-20, Rio de Janeiro, Brasil. Rio de Janeiro: CBMET, pp. 612-619.
- BAUMANN, K. H. & KINKEL, H. 1999. Coccolithophores as Indicators of Ocean Water Masses, Surface-Water Temperature and Paleoproductivity - examples from the South Atlantic. In: FISCHER, G. & WEFER, G. (eds.). *Use of proxies in paleoceanography: examples from the South Atlantic*. Berlin: Springer-Verlag, pp. 117-144.
- BEHLING, H. 2002. South and southeast Brazilian grasslands during Late Quaternary times: a synthesis. *Palaeogeography, Palaeoclimatology, Palaeoecology*, 177(1-2), 19-27.
- BEHLING, H. & NEGRELLE, R. R. B. 2001. Tropical rain forest and climate dynamics of the Atlantic Lowland, Southern Brazil, during the Late Quaternary. *Quaternary Research*, 56, 383-389.
- BEHLING, H., PILLAR, V. & BAUERMANN, S. G. 2005. Late Quaternary grassland (Campos), gallery forest, fire and climate dynamics, studied by pollen, charcoal and multivariate analysis of the São Francisco de Assis core in western Rio Grande do Sul (southern Brazil). *Review of Palaeobotany and Palynology*, 133, 235-248.
- BEHLING, H., PILLAR, V., ORLÓCI, L. & BAUERMANN, S. G. 2004. Late quaternary *Araucaria* forest, grassland (Campos), fire and climate dynamics, studied by high resolution pollen, charcoal and multivariate analysis of the Cambará do Sul core in southern Brazil. *Palaeogeography, Palaeoclimatology, Palaeoecology*, 203(3-4), 277-297.
- BOLDRINI, I. I. 2009. A flora dos Campos do Rio Grande do Sul. In: PILLAR, V., MÜLLER, S. C., CASTILHOS, Z. M. S. & JACQUES, A. V. A. (eds.). *Campos sulinos: conservação e uso sustentável da biodiversidade*. Brasília: Ministério do Meio Ambiente, pp. 63-77.
- BOTTEZZINI, S. R., LEONHARDT, A., DINIZ, D. & ÁVILA, A. S. P. 2021. Climatic and vegetational dynamics in Southern Brazil between 47.8 and 7.4 cal ka BP: a palynological analysis. *Revista Brasileira de Paleontologia*, 24(4), 345-356.
- BRAGA, E. S. & NIENCHESKI, L. F. H. 2006. Composição das massas de água e seus potenciais produtivos na área entre o Cabo de São Tomé (RJ) e o Chui (RS). In: ROSSI-WONGTSCHOWSKI, C. L. D. B. & MADUREIRA L. S. P. (eds.). *O ambiente oceanográfico da plataforma continental e do talude na região Sudeste-Sul do Brasil*. São Paulo: EDUSP, pp. 161-218.

- CABRERA, A. L. 1994. Regiones topogeográficas Argentinas. *Enciclopedia Argentina de Agricultura y Ganadería*, 2, 1-85.
- CHIESSI, C. M., MULITZA, S., MOLLENHAUER, G., SILVA, J. B., GROENEVELD, J. & PRANGE, M. 2015. Thermal evolution of the western South Atlantic and the adjacent continent during termination 1. *Climate of the Past*, 11(6), 915-929.
- CRUZ JUNIOR., F. W., BURNS, S. J., KARMANN, I., SHARP, W. D., VUILLE, M., CARDOSO, A. O., FERRARI, J. A., DIAS, P. L. S. & VIANA, J. O. 2005. Insolation-driven changes in atmospheric circulation over the past 116,000 years in subtropical Brazil. *Nature*, 434(7029), 63-66.
- D'AQUINO, C. A., NETO, J. S. A., BARRETO, G. A. M. & SCHETTINI, C. A. F. 2011. Caracterização oceanográfica e do transporte de sedimentos em suspensão no estuário do Rio Mampituba, SC. *Revista Brasileira de Geofísica*, 29(2), 217-230.
- DALE, B. 1976. Cyst formation, sedimentation and preservation: factors affecting dinoflagellate assemblages in recent sediments from Trondheim fjord, Norway. *Review of Palaeobotany and Palynology*, 22, 39-60.
- DALE, B. 1996. Dinoflagellate cysts ecology: modeling and geological applications. In: JANSONIUS, J. & MCGREGOR, D. C. (eds.). *Palynology: principles and applications*. Dallas: American Association of Stratigraphic Palynologists Foundation, pp. 1249-1275.
- DE MASI, M. A. N. 1999. *Prehistoric hunter-gatherer mobility on the southern Brazilian coast: Santa Catarina Island*. Stanford: Stanford University.
- DIAZ, A. F., STUDZINSKI, C. D. & MECOSO, C. R. 1998. Relationships between precipitation anomalies in Uruguay and southern Brazil and sea surface temperature in the Pacific and Atlantic oceans. *Journal of Climate*, 11(2), 251-271.
- DINIZ, D. & MEDEANIC, S. 2012. Palynomorph records from the core of Rio Grande Cone, Brazil: Approaches for palaeoenvironmental and palaeoclimatic reconstructions in the middle Holocene. *Journal of Coastal Research*, 29(6), 1351-1360.
- DUPONT, L. M., SCHLÜTZ, F., EWAH, C. T., JENNERJAHN, T. C., PAUL, A. & BEHLING, H. 2010. Two-step vegetation response to enhanced precipitation in Northeast Brazil during Heinrich Event 1. *Global Changes Biology*, 16(6), 1647-1660.
- DUQUE-CASTAÑO, M. L., LEONHARDT, A. & PIVEL, M. A. G. 2019. Morphometric analysis in the shells of the planktonic foraminifera *orbulina* universa: a source for paleoceanographic information? *Brazilian Journal of Oceanography*, 67, 1-17.
- FAEGRI, K. & IVERSEN, J. 1975. *The textbook of pollen analysis*. Oxford: Blackwell Scientific Publications.
- FERREIRA, N. S. 1996. Zona de convergência intertropical. In: *Climanálise (org.). Clima análise - Especial, Edição comemorativa de 10 anos*. Cachoeira Paulista: MCT/INPE-CPTEC.
- FLORES, J. A., BÁRCENA, M. A. & SIERRA, F. J. 2000. Ocean-surface and wind dynamics in the Atlantic Ocean off Northwest Africa during the last 140,000 years. *Palaeogeography, Palaeoclimatology, Palaeoecology*, 161, 459-478.
- GONÇALVES, J. F. & LEONHARDT, A. 2016. Contribuição dos coccolitoforídeos para o aporte de carbonato de cálcio durante o Último Máximo Glacial na Margem Continental Sul Brasileira. *Quaternary and Environmental Geosciences*, 7(1-2), 1-5.
- GONÇALVES, J. F. & LEONHARDT, A. 2021a. A influência dos processos de fundo sobre um registro fóssil de coccolitoforídeos na Bacia de Pelotas. *Anuário do Instituto de Geociências*, 44, 36784.
- GONÇALVES, J. F. & LEONHARDT, A. 2021b. Mecanismos de fertilização inferidos através do registro de coccolitoforídeos durante o Quaternário Tardio na margem continental sul-brasileira. *Revista Brasileira de Paleontologia*, 25(1), 76-89.
- GONZÁLEZ, C. & DUPONT, L. M. 2009. Tropical salt marsh succession as sea-level indicator during Heinrich events. *Quaternary Science Reviews*, 28, 939-946.
- GONZÁLEZ-SILVEIRA, A., SANTAMARÍA-DEL-ANGEL, E. & MILÁN-NÚÑEZ, R. 2006. Spatial and temporal variability of the Brazil-Malvinas Confluence and the La Plata Plume as seen by SeaWiFS and AVHRR imagery. *Journal of Geophysical Research*, 111, C06010.
- GRILL, S. C. & QUATROCCHIO, M. E. 1996. Fluctuaciones eustáticas durante el Holoceno a partir del registro de paleomicroplankton, Arroyo Napostá Grande, Sur de la Provincia de Buenos Aires. *Ameghiniana*, 33, 435-442.
- GRIMM, A. M. & TEDESCHI, R. G. 2009. ENSO and extreme rainfall events in South America. *Journal of Climate*, 22(7), 1589-1609.
- GRIMM, E. C. 1993. *TILIA v2.0 (Computer Software) Illinois State Museum*. Springfield: Research and Collection Center.
- GU, F., CHIESSI, C. M., ZONNEVELD, K. A. F. & BEHLING, H. 2018. Late Quaternary environmental dynamics inferred from marine sediment core GeoB6211-2 off southern Brazil. *Palaeogeography, Palaeoclimatology, Palaeoecology*, 496, 48-61.
- GU, F., CHIESSI, C. M., ZONNEVELD, K. A. F. & BEHLING, H. 2019. Shifts of the Brazil-Falklands/Malvinas Confluence in the western South Atlantic during the latest Pleistocene-Holocene inferred from dinoflagellate cysts. *Palynology*, 43(1), 483-493.
- GU, F., ZONNEVELD, K. A. F., CHIESSI, C. M., ARZ, H. W., JÜRGEN, P. & BEHLING, H. 2017. Long-term vegetation, climate and ocean dynamics inferred from a 73, 500 years old marine sediment core (GeoB2107-3) off southern Brazil. *Quaternary Science Reviews*, 172, 55-71.
- HUECK, K. 1966. *Die Wälder Südamerikas*. Stuttgart: Fischer-Verlag.
- IBGE (Instituto Brasileiro de Geografia e Estatística). 2004. *Mapa da vegetação do Brasil e mapa de biomas do Brasil* [online]. Rio de Janeiro: IBGE. Available at: <https://www.ibge.gov.br/geociencias/informacoesambientais/15842biomas.html?=&t=o-que-e> [Accessed: 2021 May 20].
- JACOBEL, A. W., MCMANUS, J. F., ANDERSON, R. F. & WINCKLER, G. 2017. Climate-related response of dust flux to the central equatorial Pacific over the past 150 kyr. *Earth and Planetary Science Letters*, 457, 160-172.
- KJERFVE, B. 1986. Comparative oceanography of coastal lagoons. *Estuarine Variability*, 63-81.
- KLEIN, R. M. 1978. Mapa fitogeográfico do estado de Santa Catarina. In: REITZ, R. (ed.). *Flora ilustrada Catarinense*. Itajaí: Herbário Barbosa Rodrigues, pp. 1-24.
- KLEIN, R. M. 1979. Ecologia da flora e vegetação do Vale Itajaí. *Sellowia*, 31(31), 11-164.

- KOCH, C. & YOUNG, J. R. 2007. A simple weighing and dilution technique for determining absolute abundances of coccoliths from sediment samples. *Journal of Nannoplankton Research*, 29(1), 67-69.
- KOHFELD, K. E., GRAHAM, R. M., BOER, A. M., SIME, L. C., WOLFF, E. W., LE QUÉRÉ, C. & BOPP, L. 2013. Southern Hemisphere westerly wind changes during the Last Glacial Maximum: paleo-data synthesis. *Quaternary Science Reviews*, 68, 76-95.
- LANTZSCH, H., HANEBUTH, T. J. J. & CHIESSI, C. M. 2014. The high-supply, current-dominated continental margin of southeastern South America during the late quaternary. *Quaternary Research*, 81, 339-354.
- LASKAR, J., ROBUTEL, P., JOUTEL, F., GASTINEAU, M., CORREIA, A. C. M. & LEVRARD, B. 2004. A long-term numerical solution for the insolation quantities of the Earth. *Astronomy & Astrophysics*, 428(1), 261-285.
- LEAL, M. G. & LORSCHTEITER, M. L. 2007. Plant succession in a forest on the Lower Northeast Slope of Serra Geral, Rio Grande do Sul, and Holocene palaeoenvironments, Southern Brazil. *Acta Botanica Brasílica*, 21(1), 1-10.
- LEONHARDT, A. & LORSCHTEITER, M. L. 2010. The last 25,000 years in the Eastern Plateau of Southern Brazil according to Alpes de São Francisco record. *Journal of South American Earth Sciences*, 29, 454-46.
- LEONHARDT, A. & LORSCHTEITER, M. L. 2007. Palinomorfos do perfil sedimentar de uma turfeira em São Francisco de Paula, Planalto Leste do Rio Grande do Sul, Sul do Brasil. *Revista Brasileira Botânica*, 33, 47-59.
- LEONHARDT, A. & LORSCHTEITER, M. L. 2008. Pólen de gimnospermas e angiospermas do perfil sedimentar de uma turfeira em São Francisco de Paula, Planalto Leste do Rio Grande do Sul, Sul do Brasil. *Revista Brasileira Botânica*, 31(4), 645-658.
- LISIECKI, L. E. & STERN, J. V. 2016. Regional and global benthic  $\delta^{18}\text{O}$  stacks for the last glacial cycle. *Paleoceanography*, 31(10), 1368-1394.
- LOITZEMBAUER, E. & MENDES, C. A. B. 2016. Integração da gestão de recursos hídricos e da zona costeira em Santa Catarina: a zona de influência costeira nas bacias dos rios Mampituba, Araranguá, Tubarão e Tijucas, SC. *Revista Brasileira de Recursos Hídricos*, 21(2), 466-477.
- LOPES, R. P., BONETTI, C., SANTOS, G. S., GOMEZ-PIVEL, M. A., PETRÓ, S. M., CARON, F. & BONETTI, J. 2021. Late Pleistocene sediment accumulation in the lower slope off the Rio Grande terrace, southern Brazilian Continental Margin. *Quaternary International*, 571, 97-116.
- MAHIQUES, M. M., WAINER, I. K., BURONE, L., NAGAI, R., SOUSA, S. H., LOPES FIGUEIRA, R. C., SILVEIRA, I. C., BÍCEGO, M. C., ALVES, D. P. & HAMMER, Ø. 2009. A high-resolution Holocene record on the Southern Brazilian shelf: paleoenvironmental implications. *Quaternary International*, 206(1), 52-61.
- MARANGONI, J. C. & COSTA, C. S. B. 2009. Natural and anthropogenic effects on salt marsh over five decades in the Patos lagoon (southern Brazil). *Brazilian Journal of Oceanography*, 57(4), 345-350.
- MASETTO, E. & LORSCHTEITER, M. L. 2016. Gymnosperm and angiosperm pollen grains in Holocene sediments from a paleolagoon in the coastal plain of extreme southern Brazil. *Revista Brasileira Botânica*, 39, 709-720.
- MATHIAS, G. L., NAGAI, R. H., TRINDADE, R. I. F. & MAHIQUES, M. M. 2014. Magnetic fingerprint of the late Holocene inception of the Rio de la Plata plume onto the southeast Brazilian shelf. *Palaeogeography, Palaeoclimatology, Palaeoecology*, 415, 183-196.
- MATHIAS, G. L., ROUD, S. C., CHIESSI, C. M., CAMPOS, M. C., DIAS, B. B., SANTOS, T. P., ALBUQUERQUE, A. L. S., TOLEDO, F. A. L., COSTA, K. B. & MAHER, B. A. 2021. A multi-proxy approach to unravel late pleistocene sediment flux and bottom water conditions in the Western South Atlantic Ocean. *Paleoceanography and Paleoclimatology*, 36(4), e2020PA004058.
- MOURA, J. L. G., CAROLINA, A. & FREITAS, V. 2018. Alterações na circulação de Hadley Regional e na Alta Subtropical do Atlântico Sul em um cenário de aquecimento global. *Anuário do Instituto de Geociências da Universidade Federal do Rio de Janeiro*, 43(3), 227-239.
- MOURELLE, D. & PRIETO, A. R. 2012. Modern pollen assemblages of surface samples and their relationships to vegetation in the Campos region of Uruguay. *Review of Palaeobotany and Palynology*, 181, 22-33.
- OLIVEIRA-FILHO, A. T., BUDKE, J. C., JARENKOW, J. A., EISENLOHR, P. V. & NEVES, D. R. M. 2015. Delving into the variations in tree species composition and richness across South American subtropical Atlantic and Pampean forests. *Journal of Plant Ecology*, 8, 242-260.
- PAILLARD, D., LABEYRIE, L. & YIOU, P. 1996. Macintosh program performs time-series analysis. *Eos, Transactions American Geophysical Union*, 77(39), 379.
- PALMA, E. D. & MATANO, R. P. 2009. Disentangling the upwelling mechanisms of the South Brazil Bight. *Continental Shelf Research*, 29(11-12), 1525-1534.
- PEREIRA, L. S., ARZ, H. W., PÄTZOLD, J. & PORTILHO-RAMOS, R. C. 2018. Productivity evolution in the South Brazilian bight during the last 40,000 years. *Paleoceanography and Paleoclimatology*, 33(12), 1339-1356.
- PETERSON, R. G. & STRAMMA, L. 1991. Upper-level circulation in the South Atlantic Ocean. *Progress in Oceanography*, 26(1), 1-73.
- PETRÓ, S. M., PIVEL, M. A. G. & COIMBRA, J. C. 2021. Evidence of supra-lysoclinal dissolution of pelagic calcium carbonate in the late Quaternary in the western South Atlantic. *Marine Micropaleontology*, 166, 102013.
- PICHA, S., ABOUCHAMI, W. & GALER, S. J. G. 2014. Lead isotopes in the eastern equatorial Pacific record quaternary migration of the south westerlies. *Earth and Planetary Science Letters*, 388, 293-305.
- PILLAR, V. D. 1997. Multivariate exploratory analysis and randomization testing with MULTIV. *Coenoses*, 12, 145-148.
- PIOLA, A. R., MATANO, R. P., PALMA, E. D., MÖLLER JUNIOR, O. O. & CAMPOS, E. J. 2005. The influence of the Plata River discharge on the western South Atlantic shelf. *Geophysical Research Letters*, 32, L01603.
- PIOLA, A. R., ROMERO, S. I. & ZAJACZKOVSKI, U. 2008. Space-time variability of the Plata plume inferred from ocean color. *Continental Shelf Research*, 28(13), 1556-1567.
- PIVEL, M. A. G., SANTAROSA, A. C. A., BARIANI, L., COSTA, K. B. & TOLEDO, F. A. L. 2011. Paleontologia: cenários de vida. In: PIVEL, M. A. G., SANTAROSA, A. C. A., BARIANI, L., COSTA, K. B. & TOLEDO, F. A. L. (eds.). *Paleoprodutividade na Bacia de Santos nos últimos 15 mil anos*. Rio de Janeiro: Editora Interciência, pp. 331-341.

- RAZIK S., GOVIN, A., CHIESSI, C. M. & VON DOBENECK, T. 2015. Depositional provinces, dispersal and origin of terrigenous sediments along the SE South American continental margin. *Marine Geology*, 363, 261-272.
- REIMER, P. J., BARD, E., BAYLISS, A., BECK, J. W., BLACKWELL, P. G., BRONK RAMSEY, C., BUCK, C. E., CHENG, H., EDWARDS, R. L., FRIEDRICH, M., GROOTES, P. M., GUILDERTSON, T. P., HAFLIDASON, H., HAJDAS, I., HATT, C., HEATON, T. J., HOFFMANN, D. L., HOGG, A. G., HUGHEN, K. A., KAISER, K. F., KROMER, B., MANNING, S. W., NIU, M., REIMER, R. W., RICHARDS, D. A., SCOTT, E. M., SOUTHON, J. R., STAFF, R. A., TURNEY, C. S. M. & VAN DER PLICHT, J. 2013. IntCal13 and Marine13 radiocarbon age calibration curves 0 to 50,000 years cal BP. *Radiocarbon*, 55(4), 1869-1887.
- ROTH, L. & LORSCHETTER, M. L. 2013. Bryophyte and pteridophyte spores and gymnosperm pollen grains of sedimentary profiles from two forest areas of the Southern Brazilian Coastal Plain. *Revista Brasileira Botânica*, 36, 99-110.
- SANTOS, A., CARVALHO, M. A., OLIVEIRA, A. D. & MENDONÇA FILHO, J. G. 2017. Paleoenvironmental changes and influence on *Operculodinium centrocarpum* during the Quaternary in the Campos Basin, southwestern Brazil. *Journal of South American Earth Sciences*, 80, 255-271.
- SCHNEIDER, T., BISCHOFF, T. & HAUG, G. H. 2014. Migration and dynamics of the intertropical convergence zone. *Nature*, 513, 45-53.
- SOUZA, R. B. & ROBINSON, I. S. 2004. Lagrangian and satellite observations of the Brazilian coastal current. *Continental Shelf Research*, 24, 241-262.
- SPRATT, R. M. & LISIECKI, L. E. 2016. *A Late Pleistocene sea level stack*. *Climate of the Past*, 12, 1079-1092 [online]. Boulder: NOAA Paleoclimatology Program. Available at [https://www1.ncdc.noaa.gov/pub/data/paleo/contributions\\_by\\_author/spratt2016/spratt2016.txt](https://www1.ncdc.noaa.gov/pub/data/paleo/contributions_by_author/spratt2016/spratt2016.txt) [Accessed: 2021 May 12].
- STOCKMARR, L. 1971. Tablets with spores used in absolute pollen analysis. *Polen et Spores*, 13, 615-621.
- STRAMMA, L. & ENGLAND, M. 1999. On the water masses and mean circulation of the South Atlantic Ocean. *Journal Geophysical Research*, 104(C9), 20863-20883.
- STUIVER, M. & REIMER, P. J. 1993. Extended <sup>14</sup>C data base and revised Calib 3.0 <sup>14</sup>C age calibration program. *Radiocarbon*, 35(1), 215-230.
- TOLEDO, F. A. L., CACHÃO, M., COSTA, K. B. & PIVEL, M. A. G. 2007. Planktonic foraminifera, calcareous nannoplankton and ascidian variations during the last 25 kyr in the Southwestern Atlantic: a paleoproductivity signature? *Marine Micropaleontology*, 64, 67-79.
- TOLEDO, F. A. L., COSTA, K. B., PIVEL, M. A. G. & CAMPOS, E. J. D. 2008. Tracing past circulation changes in the western South Atlantic based on planktonic foraminifera. *Revista Brasileira de Paleontologia*, 11(3), 169-178.
- VOIGT, I., CHIESSI, C. M., PRANGE, M., MULITZA, S., GROENEVELD, J., VARMA, V. & HENRICH, R. 2015. Holocene shifts of the southern westerlies across the South Atlantic. *Paleoceanography*, 30, 39-51.
- WAELEBROECK, C., LABEYRIE, L., MICHEL, E., DUPLESSY, J. C., MCMANUS, J., LAMBECK, K., BALBON, E. & LABRACHERIE, M. 2002. Sea-level and deep water temperature changes derived from benthic foraminifera isotopic records. *Quaternary Science Review*, 21, 295-305.
- WAINER, I. & TASCETTO, A. S. 2006. Climatologia na região entre o Cabo de São Tomé (RJ) e o Chui (RS). Diagnóstico para os períodos relativos aos levantamentos pesqueiros do Programa REVIZEE. In: ROSSI-WONGTSCHOWSKI C. L. B. & MADUREIRA L. S. P. (eds.). *O ambiente oceanográfico da plataforma continental e do talude na região sudeste-sul do Brasil*. São Paulo: EDUSP, pp. 121-160.
- WANG, D., GOUHIER, T. C., MENGE, B. A. & GANGULY, A. R. 2015. Intensification and spatial homogenization of coastal upwelling under climate change. *Nature*, 518, 390-394.
- ZONNEVELD, K. A. F., MARRET, F., VERSTEEGH, G. J. M., BOGUS, K., BONNET, S., BOUIMETARHAN, I., CROUCH, E., VERNAL, A., ELSHANAWANY, R., EDWARDS, L., ESPER, O., FORKE, S., GRØSFJELD, K., HENRY, MARYSE., HOLZWARTH, U., KIELT, J. F., KIM, S. Y., LADOUCEUR, S., LEDU, D., CHEN, L., LIMOGES, A., LONDEIX, L., LU, S. H., MAHMOUD, M. S., MARINO, G., MATSOUKA, K., MATTHIESSEN, J., MILDENHAL, D. C., MUDIE, P., NEIL, H. L., POSPELOVA, V., QI, Y., RADI, T., RICHEROL, T., ROCHON, A., SANGIORGI, F., SOLINAC, S., TURON, J. L., VERLEYE, T., WANG, Y., WANG, Z. & YOUNG, M. 2013. Atlas of modern dinoflagellate cyst distribution based on 2405 data points. *Review of Palaeobotany and Palynology*, 191, 1-197.